JOURNAL OF PROPULSION AND POWER
Vol. 10, No. 4, July–Aug. 1994

Formulation, Predictions, and Sensitivity Analysis of a Pyrotechnically Actuated Pin Puller Model

Keith A. Gonthier* and Joseph M. Powers†
University of Notre Dame, Notre Dame, Indiana 46556

This article presents an analysis for pyrotechnic combustion and pin motion in the NASA Standard Initiator (NSI) actuated pin puller. The conservation principles and constitutive relations for a multiphase system are posed and reduced to a set of five ordinary differential equations which are solved to predict the system's performance. The model tracks the interactions of the unreacted, incompressible solid pyrotechnic, incompressible condensed phase combustion products, and gas phase combustion products. Predicted pressure histories for the firing of an NSI into 1) the pin puller device, 2) a 10 cm³ closed vessel, and 3) an apparatus known as the Dynamic Test Device compare well with experimental results. A sensitivity analysis reveals large regions in parameter space where system performance is insensitive to particular parametric values; smaller regions of high sensitivity are also found.

Introduction

PYROTECHNICALLY actuated devices are used in numerous aerospace applications. Their ability to rapidly deliver high pressures renders them the tool of choice to perform such functions as pulling pins, exploding bolts, and cutting cables. In order to better design these devices, it is necessary to understand the interaction between the combustion process and the operation of the device; in order to quantify this understanding, it is necessary to develop models. Due to the many complexities associated with a comprehensive model (three dimensionality, time-dependency, complex reaction kinetics, etc.), simple models have been the preferred choice of many researchers.[1–4] These models often use chemical equilibrium calculations to predict the composition of the combustion products and model the combustion rate by a simple empirical expression. They also require a number of additional assumptions; e.g., a well-stirred constant volume reactor is typically simulated.

The focus of this article is to present a methodology that can be used for modeling pyrotechnic combustion driven systems. Many of the assumptions listed above are adopted; additionally, the study is placed in the context of multiphase flow theory.[5–7] The primary advantage of this approach is that it offers a rational framework for 1) accounting for systems in which unreacted solids and condensed phase products form a large fraction of the mass and volume of the combined system, thus avoiding the restrictions of the dusty gas limit; and 2) accounting for the transfer of mass, momentum, and energy both within and between phases. The existing archival literature contains few, if any, sources which model pyrotechnically-driven systems; we believe this article identifies a way in which pyrotechnic combustion modeling can be used to predict the behavior of simple devices which have important engineering applications.

The utility of the methodology is illustrated by applying it to a device which is well-characterized by experiments: the NASA Standard Initiator (NSI) driven pin puller. Figure 1 depicts a cross section of a pyrotechnically actuated pin puller in its unretracted state.[8] The primary pin, which will be referred to as the pin for the remainder of this article, is driven by gases generated by the combustion of a pyrotechnic which is contained within the NSI. The NSI was originally developed as an initiator for solid rocket motors, but has been adapted for other tasks such as this. Two NSIs are tightly threaded into the device's main body. Only one NSI need operate for the proper functioning of the pin puller; the second is a safety precaution in the event of failure of the first. The pyrotechnic consists of a 114-mg mixture of zirconium fuel (54.7-mg Zr) and potassium perchlorate oxidizer (59.3-mg $KClO_4$). Initially, a thin diaphragm tightly encloses the pyrotechnic. Combustion is initiated by the transfer of heat from an electric bridgewire to the pyrotechnic. Upon ignition, the pyrotechnic undergoes rapid chemical reaction producing both condensed phase and gas phase products. The high-pressure products accelerate the combustion rate, burst the confining diaphragm, then vent through the port into the gas expansion chamber. Once in the chamber, the high-pressure gas first causes a set of shear pins to fail, then pushes the pin. After the pin is stopped by crushing an energy absorbing cup, the operation of the device is complete. Peak pressures within the expansion chamber are typically around 50.0 MPa; completion of the stroke requires approximately 0.5 ms.[8]

This article gives 1) a description of the model including both the formulation of the model in terms of the mass, momentum, and energy principles supplemented by geometrical and constitutive relations, and the mathematical reductions used to refine the model into a form suitable for numerical computations; 2) model predictions and comparisons with experimental results; and 3) results showing the parametric sensitivity of the model.

Model Description

Assumptions adopted for the model are as follows. As depicted in Figs. 2a and 2b, the combined system is taken to consist of three subsystems: 1) incompressible solid pyrotechnic reactants s, incompressible condensed phase products cp, and gas phase products g. The surroundings are taken to consist of an isothermal cylindrical vessel bounded on one end by a movable, frictionless, adiabatic pin. Mass can be transferred within the combined system from the solid pyrotechnic to both the condensed phase and gas phase products. There is no mass exchange between the combined system and the surroundings. The only heat exchange within the combined system is from the condensed phase products to the gas phase products. The rate of this heat transfer is assumed to be sufficiently large such that thermal equilibrium between the product subsystems exists. Both product subsystems are allowed to interact across the system boundary in the form of heat exchanges. The gas phase products are allowed to do

Received Aug. 2, 1993; revision received Dec. 15, 1993; accepted for publication Dec. 21, 1993.

*Graduate Research Assistant. Student Member AIAA.
†Assistant Professor, Department of Aerospace and Mechanical Engineering. Member AIAA.

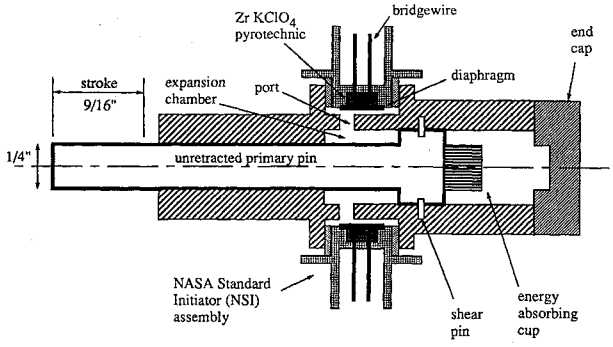

Fig. 1 Cross-sectional view of a pyrotechnically actuated pin puller (drawing not to scale).

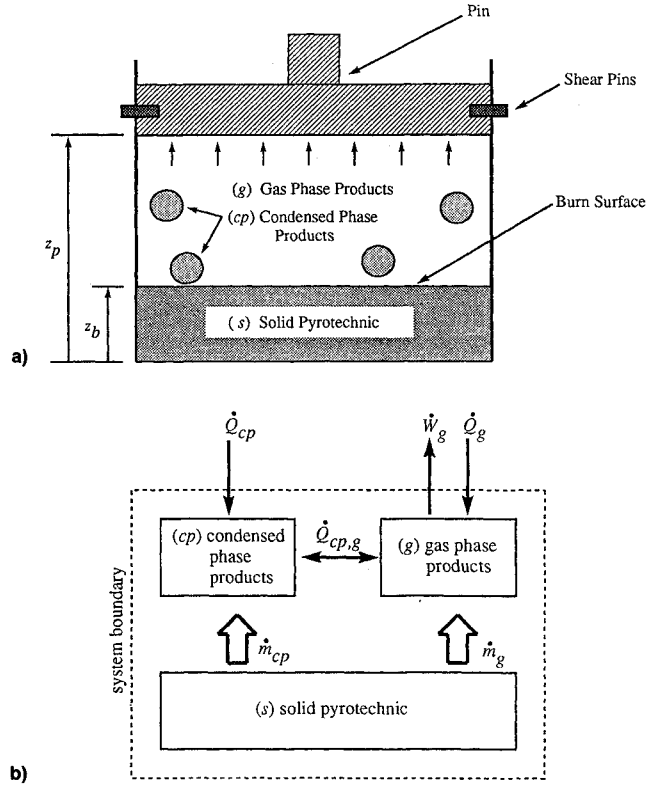

Fig. 2 a) Hypothetical configuration of pin puller device used in the model development and b) mass, heat transfer, and work interactions between subsystems and the surroundings.

expansion work on the surroundings. No work exchange between subsystems is allowed. Spatial variations within subsystems are neglected; consequently, all variables are only time-dependent, and the combined system is modeled as a well-stirred reactor. The kinetic energy of the subsystems is ignored, while an accounting is made of the kinetic energy of the bounding pin. Body forces are neglected.

To model the combustion in the pyrotechnic, we choose a standard model which holds that the rate of linear regression of the solid pyrotechnic is a function of the gas phase pressure, namely, $dz_b/dt = bP_g^n$, where z_b is the instantaneous position of the burn surface, t is time, P_g is the pressure of the gas phase combustion products, and b and n are experimentally determined constants. This form for the burn rate is commonly used in solid propellant combustion modeling,[9] and also models the burn rate of the pyrotechnic $TiH_{0.2}/KClO_4$ for pressures in the range of 0.5–4.0 MPa.[10] In the absence of data for $Zr/KClO_4$, we have chosen values for b and n so that the predictions of our model correlate with experimental pressure-time data. It is emphasized that these predictions should be performed with a constitutive equation based directly on combustion data from $Zr/KClO_4$ if such data become available; such predictions would provide a better test of the model's validity.

Predictions from the equilibrium thermochemistry code CET89[11] for the constant volume complete combustion of the $Zr/KClO_4$ mixture are used to estimate the product mass fractions. It is assumed that the mass fractions of product species are known constants predicted by the constant volume combustion calculation. For this calculation, a volume of 5 cm^3 was chosen since it represents an intermediate value for the initial volumes of devices for which pressure-time data exists: a pin puller device (0.83 cm^3), a 10-cm^3 closed vessel, and a Dynamic Test Device (1.24 cm^3). This assumption naturally introduces some error as the product species mass fractions can vary with changes in pressure, temperature, and volume encountered during the devices' operation. However, except for times (<0.01 ms) which are small relative to typical device operation times (~0.5 ms), the pressure and temperature are such that the mean specific heat and molecular weight are essentially constant. These quantities differ by a factor near 2 at early times, but the integrated effect of this error is small. The advantage in this approach is that the product gases can be modeled as a single gas; consequently, the equations, which with variable mass fractions form a nonlinear differential-algebraic system of very large dimension, can be reduced to a much simpler nonlinear system of five differential equations.

The component gases are taken to be ideal with temperature-dependent specific heats. Such an assumption may introduce some error at elevated pressures as has been recently documented for similar systems.[12] The specific heats are in the form of fourth-order polynomial curve fits given by the CET89 code and are not repeated.

Using principles of mixture theory, a set of mass and energy evolution equations can be written for each subsystem. These equations are coupled with an equation of motion for the pin to form a set of ordinary differential equations:

$$\frac{d}{dt}(\rho_s V_s) = -\rho_s A_p r \tag{1}$$

$$\frac{d}{dt}(\rho_{cp} V_{cp}) = \eta_{cp}\rho_s A_p r \tag{2}$$

$$\frac{d}{dt}(\rho_g V_g) = (1 - \eta_{cp})\rho_s A_p r \tag{3}$$

$$\frac{d}{dt}(\rho_s V_s e_s) = -\rho_s e_s A_p r \tag{4}$$

$$\frac{d}{dt}(\rho_{cp} V_{cp} e_{cp}) = \eta_{cp}\rho_s e_s A_p r - \dot{Q}_{cp,g} + \dot{Q}_{cp} \tag{5}$$

$$\frac{d}{dt}(\rho_g V_g e_g) = (1 - \eta_{cp})\rho_s e_s A_p r + \dot{Q}_{cp,g} + \dot{Q}_g - \dot{W}_g \tag{6}$$

$$m_p \frac{d^2}{dt^2}(z_p) = F_p \tag{7}$$

The independent variable in Eqs. (1–7) is t. Dependent variables are the gas phase density ρ_g; the internal energies per unit mass e_s, e_{cp}, e_g; the volumes V_s, V_{cp}, V_g; the pin position z_p; the pyrotechnic burn rate r; the rate of heat transfer from the condensed phase products to the gas phase products $\dot{Q}_{cp,g}$; the rates of heat transfer from the surroundings to the condensed phase and gas phase product subsystems $\dot{Q}_{cp}$, $\dot{Q}_g$; the rate of work done by the gas phase products in moving the pin $\dot{W}_g$; and the net force on the pin F_p. Constant parameters are the unreacted solid pyrotechnic density ρ_s; the condensed phase product density ρ_{cp}; the mass fraction of the products which are in the condensed phase η_{cp}; the pin cross-sectional area A_p, which is also the area of the burning surface; and the mass of the pin m_p.

Equations (1–3) describe the evolution of mass of the solid pyrotechnic, condensed phase products, and gas phase products, respectively. Equations (4–6) describe the evolution of energy for the solid pyrotechnic, condensed phase products, and gas phase products, respectively. Equation (7) is the equation of motion for the pin.

Geometrical and constitutive relations used to close Eqs. (1–7) are as follows:

$$V = V_s + V_{\rm cp} + V_g \tag{8}$$

$$z_p = (V/A_p) \tag{9}$$

$$P_g = \rho_g R T_g \tag{10}$$

$$r[P_g] = \frac{{\rm d}z_b}{{\rm d}t} = bP_g^n \tag{11}$$

$$e_s[T_s] = \sum_{i=1}^{N_s} Y_{s_i} e_{s_i}[T_s] \tag{12}$$

$$e_{\rm cp}[T_{\rm cp}] = \sum_{i=1}^{N_{\rm cp}} Y_{{\rm cp}_i} e_{{\rm cp}_i}[T_{\rm cp}] \tag{13}$$

$$e_g[T_g] = \sum_{i=1}^{N_g} Y_{g_i} e_{g_i}[T_g] \tag{14}$$

$$c_{v_s}[T_s] = \sum_{i=1}^{N_s} Y_{s_i} \frac{\rm d}{{\rm d}T_s} (e_{s_i}[T_s]) \tag{15}$$

$$c_{v_{\rm cp}}[T_{\rm cp}] = \sum_{i=1}^{N_{\rm cp}} Y_{{\rm cp}_i} \frac{\rm d}{{\rm d}T_{\rm cp}} (e_{{\rm cp}_i}[T_{\rm cp}]) \tag{16}$$

$$c_{v_g}[T_g] = \sum_{i=1}^{N_g} Y_{g_i} \frac{\rm d}{{\rm d}T_g} (e_{g_i}[T_g]) \tag{17}$$

$$\dot{Q}_{{\rm cp},g}[T_{\rm cp}, T_g] = h_{{\rm cp},g} A_{\rm cp} (T_{\rm cp} - T_g) \tag{18}$$

$$\dot{Q}_{\rm cp} = \dot{Q}_{\rm cp}[V, V_s, T_{\rm cp}] \tag{19}$$

$$\dot{Q}_g = \dot{Q}_g[V, V_s, T_g] \tag{20}$$

$$\dot{W}_g = P_g \frac{{\rm d}V}{{\rm d}t} \tag{21}$$

$$F_p = \begin{cases} 0 & \text{if} \quad P_g A_p < F_{\rm crit} \\ P_g A_p & \text{if} \quad P_g A_p \geq F_{\rm crit} \end{cases} \tag{22}$$

Here, and throughout this article, brackets [ ] are used to denote a functional dependence on the enclosed variable. Equations (8) and (9) are geometrical constraints. Here, V is the volume of the combined system. Equation (10) is a thermal equation of state for the gas phase products. Occurring in this expression are the gas phase pressure P_g, the gas phase temperature T_g, and the ideal gas constant for the gas phase products R (the quotient of the universal gas constant and the mean molecular weight of the product gases). The pyrotechnic burn rate r is given by Eq. (11).

Caloric equations of state for the solid pyrotechnic, condensed phase products, and gas phase products are given by Eqs. (12–14), respectively. Here, T_s is the temperature of the solid pyrotechnic, and $T_{\rm cp}$ is the temperature of the condensed phase products. Also, Y_{s_i}, $Y_{{\rm cp}_i}$, Y_{g_i}, N_s, $N_{\rm cp}$, and N_g are the constant mass fractions and number of component species of solid pyrotechnic, condensed phase product, and gas phase product species, respectively. The subscript i denotes an individual species. Since for both ideal gases and condensed phase species, the internal energy is only a function of temperature, the specific heat at constant volume for the solid pyrotechnic c_{v_s}, the condensed phase products $c_{v_{\rm cp}}$, and the gas phase products c_{v_g}, can be obtained via term-by-term differentiation of the caloric equations of state with respect to their temperature. Expressions for the specific heats at constant volume are given by Eqs. (15–17).

Equation (18) gives an expression for the rate of heat transfer from the condensed phase products to the gas phase products. In this expression, $h_{{\rm cp},g}$ is a constant heat transfer parameter, and $A_{\rm cp}$ is the surface area of the condensed phase products. The term $h_{{\rm cp},g} A_{\rm cp}$ is assumed large for this study. The functional dependencies of the heat transfer rates between the surroundings and the product subsystems are given by Eqs. (19) and (20). These rates are considered to be dependent upon their respective product subsystem temperatures and are parameterized by the constant temperature of the vessel's wall. The functional form of these models will be given below.

Equation (21) models pressure-volume work done by the expanding gas in moving the pin. Equation (22) models the force on the pin due to the gas phase pressure and a restraining force due to the shear pins which are used to initially hold the pin in place. Here, $F_{\rm crit}$ is the critical force necessary to cause shear pin failure. The work associated with shearing the pin is not considered.

Due to the assumption of a large heat transfer rate between the condensed phase and gas phase product subsystems (i.e., $h_{{\rm cp},g} A_{\rm cp} \to \infty$), the product subsystems remain in thermal equilibrium for all time. Therefore, we take $T_p \equiv T_{\rm cp} = T_g$, with T_p representing the temperature of both product subsystems. With this assumption, one can define a net rate $\dot{Q}_p$ governing the rate of heat transfer from the surroundings to the product subsystems:

$$\begin{aligned} \dot{Q}_p[V, V_s, T_p] &= \dot{Q}_{\rm cp}[V, V_s, T_p] + \dot{Q}_g[V, V_s, T_p] \\ &= hA_w[V, V_s](T_w - T_p) + \sigma A_w[V, V_s](\alpha T_w^4 - \varepsilon T_p^4) \end{aligned} \tag{23}$$

where

$$A_w[V, V_s] = 2\sqrt{(\pi/A_p)}(V - V_s) \tag{24}$$

This model accounts for both convective and radiative heat transfer. Here, h is a constant convective heat transfer coefficient, T_w is the temperature of the vessel's wall, σ is the Stefan-Boltzmann constant, α is the absorptivity of the vessel's wall, and ε is the net emissivity of the product mixture. The variable A_w is the instantaneous surface area of the vessel's lateral wall that is in contact with the product mixture. For a cylindrical vessel, A_w is related to V and V_s by Eq. (24).

Mathematical Reductions

In this section, intermediate operations are described which lead to a refined final model. The final model consists of a set of autonomous first-order ordinary differential equations of the form ${\rm d}\boldsymbol{x}/{\rm d}t = \boldsymbol{f}(\boldsymbol{x})$, where $\boldsymbol{x} = (V, V_s, V_{\rm cp}, T_p, \dot{V})^T$, and $\boldsymbol{f}$ is a vector function of the vector $\boldsymbol{x}$. Here, it has been necessary to define a new variable, $\dot{V}$, which represents the time derivative of combined system volume:

$$\dot{V} \equiv \frac{{\rm d}V}{{\rm d}t} \tag{25}$$

The goal here is to find the specific form of $\boldsymbol{f}$ and to show how all other variables can be written as functions of $\boldsymbol{x}$.

First, Eqs. (1–3) can be added to form a homogeneous differential equation expressing the conservation of the combined system's mass:

$$\frac{\rm d}{{\rm d}t} (\rho_s V_s + \rho_{\rm cp} V_{\rm cp} + \rho_g V_g) = 0 \tag{26}$$

Integrating this equation, applying initial conditions which are denoted by the subscript "0," using Eq. (8) to eliminate V_g in favor of V, V_s, and V_{cp}, and solving for ρ_g, it is found that

$$\rho_g[V, V_s, V_{cp}] = \frac{\rho_s V_{s0} + \rho_{cp} V_{cp0} + \rho_{g0} V_{g0} - \rho_s V_s - \rho_{cp} V_{cp}}{V - V_s - V_{cp}} \tag{27}$$

Now, with the assumption of a uniform temperature for the product subsystems and using Eq. (27), Eq. (10) can be used to express P_g as functions of V, V_s, V_{cp}, and T_p:

$$P_g[V, V_s, V_{cp}, T_p] = \rho_g[V, V_s, V_{cp}]RT_p \tag{28}$$

With a knowledge of P_g, Eqs. (11) and (22) can be written in the following forms, respectively:

$$r = r[V, V_s, V_{cp}, T_p] = bP_g^n[V, V_s, V_{cp}, T_p] \tag{29}$$

$$F_p = F_p[V, V_s, V_{cp}, T_p] \tag{30}$$

With the assumption that ρ_s and ρ_{cp} are constant, the remaining mass evolution equations, Eqs. (1) and (2), can be rewritten as

$$\frac{dV_s}{dt} = -A_p r[V, V_s, V_{cp}, T_p] \tag{31}$$

$$\frac{dV_{cp}}{dt} = \eta_{cp}\left(\frac{\rho_s}{\rho_{cp}}\right) A_p r[V, V_s, V_{cp}, T_p] \tag{32}$$

The energy evolution equations will now be simplified. By multiplying Eq. (1) by e_s and subtracting this result from Eq. (4), one determines that

$$\frac{de_s}{dt} = 0 \tag{33}$$

Thus, in accordance with the assumption of no heat transfer to the solid pyrotechnic subsystem, its internal energy remains constant for all time. Integrating this expression results in the following:

$$e_s = e_{s0} \tag{34}$$

The addition of Eqs. (5) and (6) results in a single expression governing the evolution of the combustion products' energy:

$$\frac{d}{dt}[\rho_{cp} V_{cp} e_{cp} + \rho_g V_g e_g] = \rho_s e_{s0} A_p r + \dot{Q}_p[V, V_s, T_p] - \dot{W}_g \tag{35}$$

Here, the net heat transfer rate given by Eq. (23) has been incorporated. Multiplying Eq. (2) by e_{cp}, multiplying Eq. (3) by e_g, and subtracting these results from Eq. (35) yields:

$$\rho_{cp} V_{cp} \frac{de_{cp}}{dt} + \rho_g V_g \frac{de_g}{dt} = (e_{s0} - \eta_{cp} e_{cp} - (1 - \eta_{cp}) e_g)\rho_s A_p r + \dot{Q}_p[V, V_s, T_p] - \dot{W}_g \tag{36}$$

Using Eqs. (16) and (17) to re-express the derivatives in terms of T_p, using the work expression given by Eq. (21) with Eq. (25) to eliminate $\dot{W}_g$, expressing all variables as functions of V, V_s, V_{cp}, and T_p, and solving for the derivative of T_p, results in the following:

$$\frac{dT_p}{dt} = \frac{(e_{s0} - \eta_{cp} e_{cp}[T_p] - (1 - \eta_{cp}) e_g[T_p])\rho_s A_p r[V, V_s, V_{cp}, T_p] + \dot{Q}[V, V_s, T_p] - P_g[V, V_s, V_{cp}, T_p]\dot{V}}{\rho_g[V, V_s, V_{cp}](V - V_s - V_{cp}) c_{v_g}[T_p] + \rho_{cp} V_{cp} c_{v_p}[T_p]} \tag{37}$$

Lastly, Eq. (7) can be split into two first-order ordinary differential equations. The first is given by the definition presented in Eq. (25). The second equation, obtained by substituting Eqs. (9), (25), and (30) into Eq. (7), is given by the following:

$$\frac{d\dot{V}}{dt} = \frac{A_p}{m_p} F_p[V, V_s, V_{cp}, T_p] \tag{38}$$

Equations (25), (31), (32), (37), and (38) form the desired set. Initial conditions are

$$V(t = 0) = V_0, \quad V_s(t = 0) = V_{s0}$$
$$V_{cp}(t = 0) = V_{cp0}, \quad T_p(t = 0) = T_0, \quad \dot{V}(t = 0) = 0 \tag{39}$$

All other quantities of interest can be obtained once these equations are solved.

Results

In this section, numerical solutions to the model equations are presented for the simulated firing of an NSI into the pin puller device. Also, predicted pressure histories for the simulated firing of an NSI into a 10-cm³ closed bomb vessel and into an apparatus known as the Dynamic Test Device will be presented in order to further corroborate model predictions with available data. The numerical algorithm used to perform the integrations was an explicit stiff ordinary differential equation solver given in the standard code LSODE. The calculation time for a single simulation was typically a few seconds on a desktop workstation.

The chemical equation used in each of the simulations, as predicted by the constant volume (5 cm³) combustion calculation performed with the CET89 chemical equilibrium code, is presented in Table 1. The parameters used are presented in Table 2.

Pin Puller Simulation

Predictions and measurements[13] of pressure histories for the pin puller are given in Fig. 3. In the experiments, one port contained the NSI and the other a pressure transducer. Here, a rapid pressure rise is predicted up to a maximum value near 56.0 MPa occurring 0.06 ms after combustion initiation; the pressure then decreases to 23.9 MPa at completion of the stroke (0.47 ms). The rapid pressure rise is attributable to gases generated during combustion. The peak pressure occurs near the time of combustion extinction, and the subsequent pressure decay is due to the combined effect of heat transfer to the surroundings and work done by the expanding gas in moving the pin. Figure 4 gives the predicted temperature history for the combustion product mixture.

Figure 5 illustrates the partitioning of the total energy of the combined system between the total internal energy of the solid pyrotechnic, the total internal energy of the combustion product mixture, the kinetic energy of the pin (labeled "work"), and the energy lost to the surroundings as heat. As combustion proceeds, the total internal energy of the solid pyrotechnic decreases. As the specific internal energy of the solid pyrotechnic is constant, the decrease in the total internal energy of the solid pyrotechnic is purely due to volumetric change. During the same time, the total internal energy of the combustion products increases to such an extent that the products contain nearly all of the combined system's energy. Very little energy is used in moving the pin or lost to the surroundings during this time. Following completion of the combustion process, about 10% of the combined system's energy is used in retracting the pin. For the particular parameters used here,

Table 1 Chemical equation used in pyrotechnic combustion simulations

$$3.8354Zr(s) + 2.7359KClO_4(s) \rightarrow 3.2661ZrO_2(cp) + 1.8287O(g) + 1.8023KCl(g) + 0.9079Cl(g) + 0.7650K(g) + 0.6830O_2(g) + 0.4625ZrO_2(g) + 0.1554KO(g) + 0.0917ZrO(g) + 0.0142ClO(g) + 0.0042K_2Cl_2(g) + 0.0024K_2(g) + 0.0015Cl_2(g) + 0.0001Zr(g)$$

Table 2 Parameters used in pyrotechnic device simulations

Parameter	Value
η_{cp}	0.42
A_p	0.64,[a] 2.0,[b], 5.07[c] cm^2
m_p	19.0,[a] 453.6[c] g
ρ_s	3.57 g/cm^3
ρ_{cp}	5.9 g/cm^3
h	1.25×10^6 g/s^3/K
σ	5.67×10^{-5} g/s^3/K
ε	0.6
α	0.6
F_{crit}	3.56×10^7 dyne
b	0.0012 (dyne/cm^2)$^{-0.74}$ cm/s
n	0.74
V_0	0.83,[a] 10.0,[b] 1.24[c] cm^3
V_{s0}	0.032 cm^3
V_{cp0}	8.44×10^{-7} cm^3
T_0	288.0 K
$\dot{V}_0$	0.0 cm^3/s

[a]Pin puller. [b]Closed bomb. [c]Dynamic Test Device.

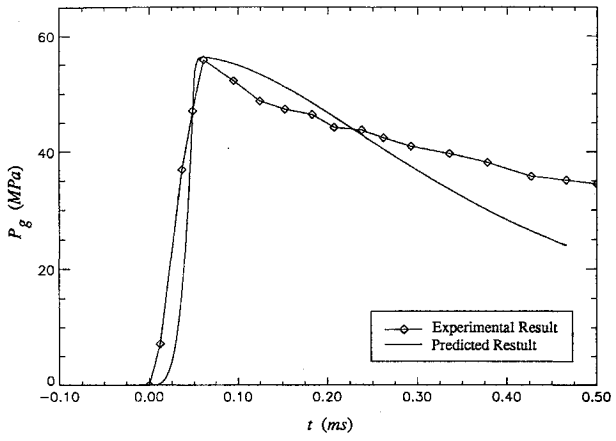

Fig. 3 Predicted and experimental pressure histories for the pin puller test.

about 1% of the combined system's energy is lost to the surroundings due to heat transfer. The predicted kinetic energy of the pin at completion of the stroke is 32.6 J. Experimentally observed values for the pin kinetic energy at completion of the stroke and stroke time are typically near 23 J and 0.50 ms, respectively. Both the higher value for the predicted pin kinetic energy and the lower value for the predicted stroke time are consistent with the fact that frictional effects, which would tend to retard the motion of the pin, have not been accounted for in the model.

Closed Bomb Simulation

Closed bomb firings are commonly used as a standard measure of the energy output of pyrotechnic cartridges. In closed bomb testing, a pyrotechnic cartridge is fired into a constant volume bomb, and the resulting pressure rise is measured with pressure transducers. A relevant NASA standard requires that the firing of an NSI into a 10-cm^3 bomb shall produce a peak pressure of 650 ± 125 psi [4.48 ± 0.86 MPa] within 5 ms.[14] The predicted pressure history for this simulation is presented in Fig. 6. Also presented in this figure are experimentally observed values.[14] Excluding work exchange

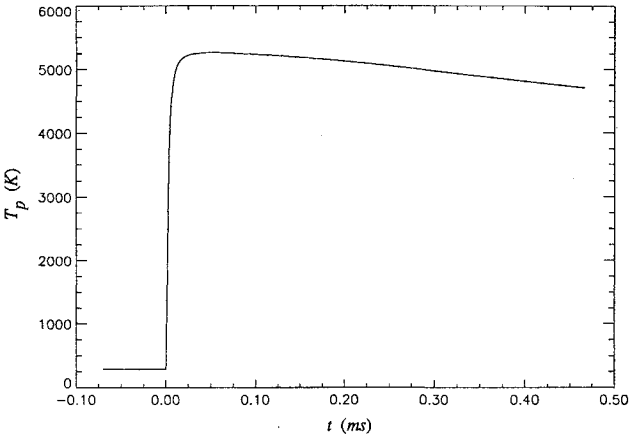

Fig. 4 Predicted temperature history for the pin puller test.

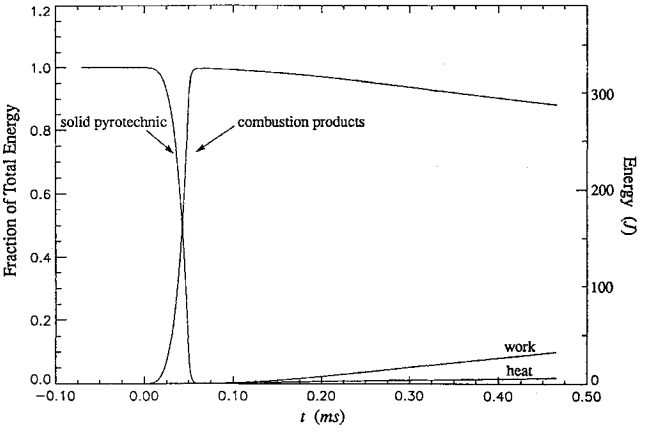

Fig. 5 Partitioning of energy for the pin puller test.

with the surroundings, the predicted trends are the same as those presented for the pin puller simulation.

Dynamic Test Device Simulation

The Dynamic Test Device is a device which was also designed to define and compare the energy production capabilities of pyrotechnic cartridges. The NSI cartridge output is delivered into a small initial free volume (1.24 cm^3) to thrust a 1-in.- (2.54-cm-) diam, 1-lb mass (453.6 g) cylindrical piston through a 1-in. (2.54-cm) stroke. The resulting pressure is measured with pressure transducers and the energy output is measured as the average kinetic energy, measured through laser velocimetry, of the piston during the stroke.

The predicted and experimental[14] pressure histories are shown in Fig. 7. Predicted trends are the same as those presented above for the pin puller simulation. The predicted average kinetic energy of the piston is 45.6 J. This compares to experimentally observed values near 30.0 J. The higher value for the predicted kinetic energy of the piston can again be considered consistent with the neglect of friction in the model.

Model Sensitivity

This section gives results showing the sensitivity of the model to variations in the burn rate parameters b and n and the heat transfer parameters h, α, and ε. For this study, we use the predicted pin puller solution as the baseline solution (baseline

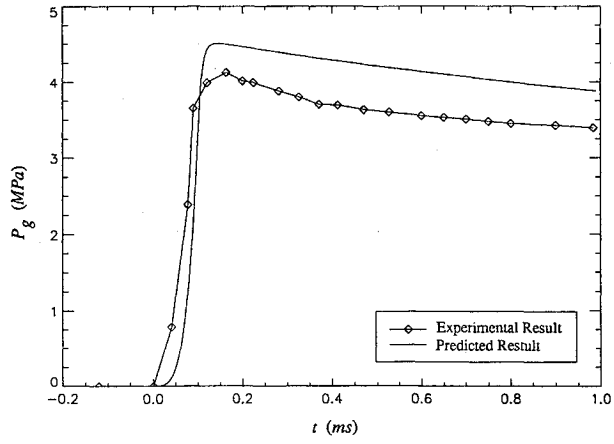

Fig. 6 Predicted and experimental pressure histories for the closed bomb test.

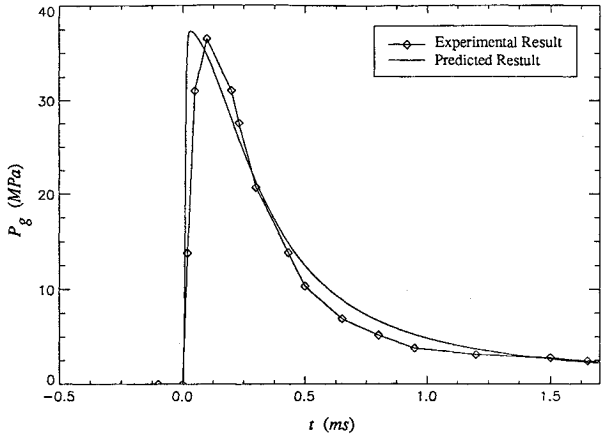

Fig. 7 Predicted and experimental pressure histories for the Dynamic Test Device test.

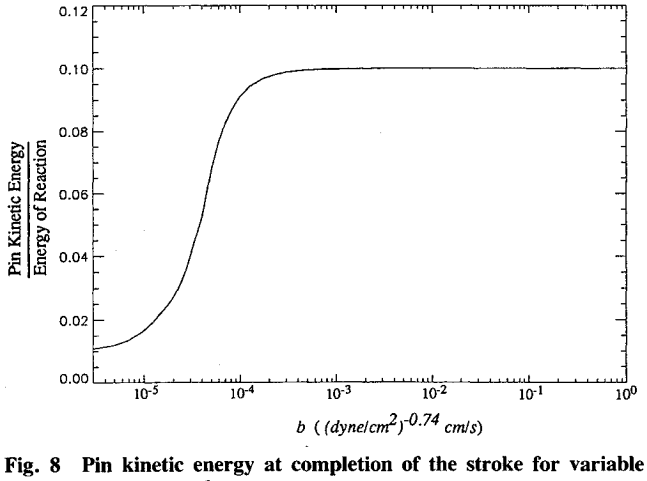

Fig. 8 Pin kinetic energy at completion of the stroke for variable burn rate parameter *b*.

parameters given in Table 2). The sensitivity of the model is determined by solving the pin puller problem and finding the parametric dependency of the pin kinetic energy at completion of the stroke.

Model sensitivity to changes in the burn rate parameters b and n is shown in Figs. 8 and 9, respectively. In these figures, the predicted kinetic energy of the pin at completion of the stroke has been nondimensionalized by the total energy released by the combustion process (326.2 J). For $b \geq 2.0 \times 10^4$ (dyne/cm^2)$^{-0.74}$ cm/s or $n \geq 0.65$, corresponding to fast burning rates, the ratio of the predicted kinetic energy of the pin at completion of the stroke to the total combustion energy approaches an approximately constant peak value of 0.10 (32.6 J). For smaller values of these parameters, corresponding to slower burning rates, the predicted kinetic energy of the pin at completion of the stroke decreases as the rate of heat transfer to the surroundings becomes more significant.

Model sensitivity to changes in the convective heat transfer coefficient h and the radiative heat transfer parameters α and ε is shown in Figs. 10 and 11, respectively. Trends observed in Fig. 10 show that for values of $h \leq 1.0 \times 10^7$ g/s^3/K, the predicted kinetic energy of the pin approaches a maximum.

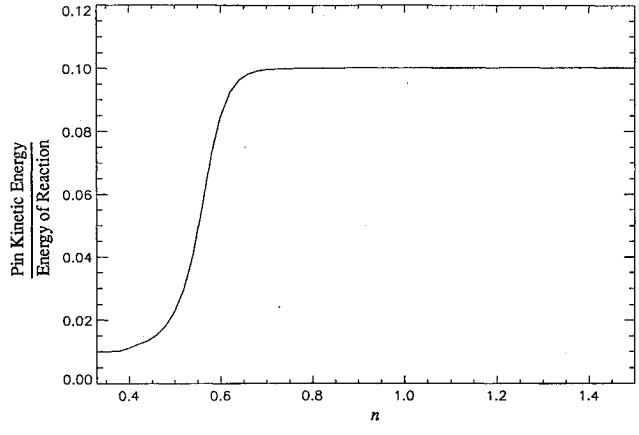

Fig. 9 Pin kinetic energy at completion of the stroke for variable burn rate parameter *n*.

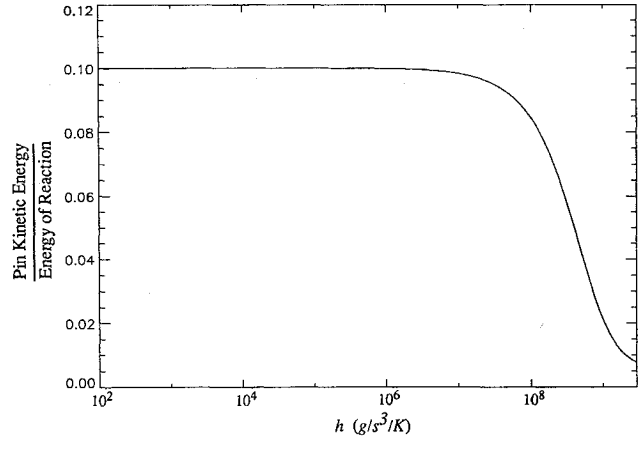

Fig. 10 Pin kinetic energy at completion of the stroke for variable convective heat transfer coefficient *h*.

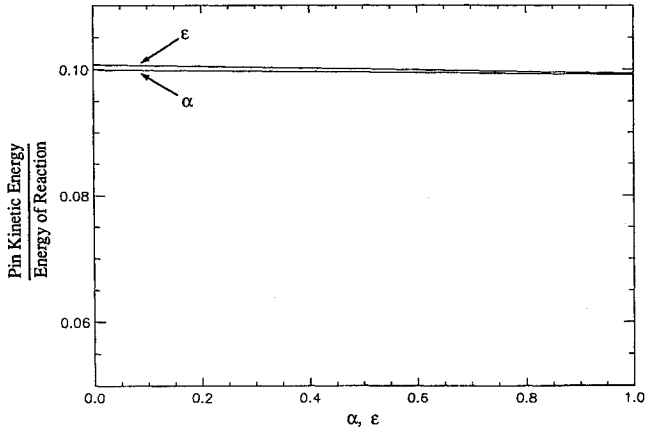

Fig. 11 Pin kinetic energy at completion of the stroke for variable absorptivity α and emissivity ε.

For larger values of this parameter, the pin kinetic energy decreases as the rate of heat transfer to the surroundings increases. Typical values of h for gas phase and liquid phase mixtures extend over a large range from 5×10^3 g/s^3/K to values in excess of 1×10^8 g/s^3/K.[15] Figure 11 shows that the model is relatively insensitive to changes in α or ε.

Conclusions

This article has presented a methodology which can be used to model dynamic events associated with the firing of pyrotechnically actuated devices. The model has demonstrated reasonable success in predicting experimentally observed time scales and pressure magnitudes associated with the operation of a pin puller device. Results of the sensitivity analysis reveal that, in order to obtain optimal pin puller performance, the burning rate of the pyrotechnic should be large and the convective rate of heat transfer from the product mixture to the surroundings should be small. Results of the sensitivity analysis further show that, outside of certain critical burn rate and convective heat transfer parameter ranges, the variable which is of actual engineering interest, namely the pin's kinetic energy, is insensitive to changes in these parameters. Consequently, it may not be necessary to have a great deal of precision in making estimates for these parameters; only certain bounds need be specified.

The model can be easily extended to relax certain modeling assumptions. Such extensions might account for nonideal gas effects, mass choking as the combustion products exit the port, variations in the equilibrium product composition with temperature and pressure, and multiple pyrotechnic grains with variable grain sizes. More advanced studies should relax the assumption of a well-stirred reactor to allow for spatial variations. This would allow one to 1) better model the interaction between product gases and condensed phase products, 2) include effects of diffusion, 3) include effects of turbulence, and 4) consider nonlinear wave dynamics. Such a step would require the solution of a set of partial differential model equations, which significantly complicates the analysis. Lastly, if accurate burn rate data for $Zr/KClO_4$ becomes available, it should be incorporated into the model.

Acknowledgments

This study was supported by the NASA Lewis Research Center under Contract NAG-1335. Robert M. Stubbs is the contract monitor. The authors recognize many helpful conversations with P. Barry Butler of the University of Iowa, Iowa City, Iowa. Additionally, many substantive comments of a referee have been adopted in our revision.

References

[1]Razani, A., Shahinpoor, M., and Hingorani-Norenberg, S. L., "A Semi-Analytical Model for the Pressure-Time History of Granular Pyrotechnic Materials in a Closed System," *Proceedings of the 15th International Pyrotechnics Seminar* (Chicago, IL), IIT Research Inst., Chicago, IL, 1990, pp. 799–813.

[2]Farren, R. E., Shortridge, R. G., and Webster, H. A., III, "Use of Chemical Equilibrium Calculations to Simulate the Combustion of Various Pyrotechnic Compositions," *Proceedings of the 11th International Pyrotechnics Seminar* (Vail, CO), IIT Research Inst., Chicago, IL, 1986, pp. 13–40.

[3]Butler, P. B., Kang, J., and Krier, H., "Modeling of Pyrotechnic Combustion in an Automotive Airbag Inflator," *Proceedings—Europyro 93, 5e Congres International de Pyrotechnie du Groupe de Travaile* (Strasbourg, France), Association Francaise de Pyrotechnie, France, 1993, pp. 61–70.

[4]Kuo, J. H., and Goldstein, S., "Dynamic Analysis of NASA Standard Initiator Driven Pin Puller," AIAA Paper 93-2066, June 1993.

[5]Baer, M. R., and Nunziato, J. W., "A Two-Phase Mixture Theory for the Deflagration to Detonation Transition (DDT) in Reactive Granular Materials," *International Journal of Multiphase Flow*, Vol. 12, No. 6, 1986, pp. 861–889.

[6]Powers, J. M., Stewart, D. S., and Krier, H., "Theory of Two-Phase Detonation—Part I: Modeling," *Combustion and Flame*, Vol. 80, Nos. 3 and 4, 1990, pp. 264–279.

[7]Powers, J. M., Stewart, D. S., and Krier, H., "Theory of Two-Phase Detonation—Part II: Structure," *Combustion and Flame*, Vol. 80, Nos. 3 and 4, 1990, pp. 280–303.

[8]Bement, L. J., Multhaup, H. A., and Schimmel, M. L., "HALOE Gimbal Pyrotechnic Pin Puller Failure Investigation, Redesign, and Qualification," NASA Langley Research Center Rept., Hampton, VA, Aug. 1991.

[9]King, M. K., "Erosive Burning of Solid Propellants," *Journal of Propulsion and Power*, Vol. 9, No. 6, 1993, pp. 785–805.

[10]Holy, J. A., "Pressure Dependent Burn Rates of $TiH_x/KClO_4$ (x = 0.2, 0.65, 1.65)," *Proceedings of the 11th International Pyrotechnics Seminar* (Vail, CO), IIT Research Inst., Chicago, IL, 1986, pp. 327–344.

[11]Gordon, S., and McBride, B. J., "Computer Program for Calculation of Complex Chemical Equilibrium Compositions, Rocket Performance, Incident and Reflected Shocks, and Chapman-Jouguet Detonations," NASA Lewis Research Center, SP-273, Cleveland, OH, March 1976.

[12]Hobbs, M. L., and Baer, M. R., "Nonideal Thermoequilibrium Calculations Using a Large Product Species Data Base," *Shock Waves*, Vol. 2, No. 3, 1992, p. 177.

[13]Bement, L. J., private communication, NASA Langley Research Center, Hampton, VA, 1992.

[14]Bement, L. J., and Schimmel, M. L., "Cartridge Output Testing: Methods to Overcome Closed Bomb Shortcomings," 1990 SAFE Symposium, San Antonio, TX, Dec. 1990.

[15]Incropera, F. P., and DeWitt, D. P., *Fundamentals of Heat and Mass Transfer*, 2nd ed., Wiley, New York, 1985, p. 8.